

# Single top-quarks at the LHC

**D B Ta on behalf of the ATLAS and CMS collaborations**

Nikhef, Science Park 105, 1098 XG Amsterdam, The Netherlands

**Abstract.** This article summarises the status of measurements of single top-quark production in all channels at the LHC for a centre-of-mass energy of 7 TeV with the full 2011 data set and for a centre-of-mass of 8 TeV for the  $t$ -channel cross-section. Results are reported from the ATLAS and CMS experiments. Both experiments also report evidence for the  $Wt$ -channel production which has never been observed before. ATLAS also sets a limit on the  $s$ -channel cross-section. So far, the measured cross sections are in good agreement with the predictions by the Standard Model.

## 1. Introduction

At the LHC, top quarks are expected to be produced singly via weak, charged-current interactions in the  $Wtb$  vertex. There are three relevant subprocesses that are distinguished by the virtuality of the exchanged  $W$  boson. The dominant process is the  $t$ -channel exchange of a virtual  $W$  ( $t$ -channel). As opposed to the case at the Tevatron, the subprocess with the second highest cross section is the associated production of an on-shell  $W$  boson and a top quark ( $Wt$ -channel). The Drell-Yan type production of a single top-quark ( $s$ -channel) has the smallest cross section. For all three channels the Feynman diagrams are depicted in Fig. 1. The approximate NNLO calculations [1, 2, 3] for all the single top-quark production processes at both 7 TeV and 8 TeV are given in Table 1 for the sum of single  $t$  and  $\bar{t}$  production. The ratio of  $t$  and  $\bar{t}$  in the  $t$ - and  $s$ -channel is roughly 2, which corresponds to the ratio of up and down valence-quarks in the colliding protons. The total cross section for single top-quark production amounts to about half of that of  $t\bar{t}$  production [4].

**Table 1.** Theoretical cross-section for the different single top-quark channels.

| centre-of-mass energy | $t$ -channel [1]     | $Wt$ -channel [2] | $s$ -channel [3] |
|-----------------------|----------------------|-------------------|------------------|
| 7 TeV                 | $64.6_{-2.0}^{+2.7}$ | $15.7 \pm 1.1$    | $4.6 \pm 0.2$    |
| 8 TeV                 | $87.8_{-1.9}^{+3.4}$ | $22.4 \pm 1.5$    | $5.6 \pm 0.2$    |

Measuring the cross section and properties of single top-quarks tests the structure of the  $Wtb$  vertex, which in the Standard Model (SM), is governed by the weak interaction. The CKM matrix element  $|V_{tb}|$  can be directly extracted from the cross-section measurement without the three fermion generations assumption, allowing to test for a 4th or higher generation hypothesis. The cross sections are also sensitive to the parton distribution functions (PDFs). The total  $t$ -channel cross-section is sensitive to the  $b$ -quark PDF, while the ratio of  $t$  and  $\bar{t}$  production cross-sections is sensitive to the up- and down-quark PDF ratio.



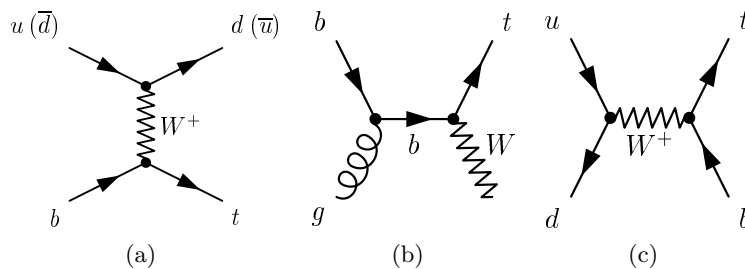


**Figure 1.** Leading-order Feynman diagrams for the three single-top channels: (a)  $t$ -channel, (b)  $Wt$ -channel and (c)  $s$ -channel.

Single top-quarks final states occur in many models of physics beyond the SM [5], for example in the production of a heavy  $W'$ -boson that decays preferentially into quarks (see ATLAS and CMS measurements in Refs. [6, 7]), in the production of a charged Higgs boson, in the decays of fourth generation or excited quarks (see Ref. [8]) or in the final state for flavour-changing neutral-current interactions (see Ref. [9]). Cross-section measurements in each individual channel are important as the different channels are sensitive to different types of physics models beyond the SM.

## 2. General physics object reconstruction and selection

The general object reconstruction and object definitions details for ATLAS [10] and CMS [11] can be found in Refs. [12, 13, 14, 15, 16] and Refs. [17, 18, 19], respectively.

In general, events are selected at ATLAS with high transverse momentum single lepton triggers (isolation from calorimeter energy depositions at trigger level is required for the 8 TeV analyses). Leptons are required to have transverse momentum,  $p_T > 25$  GeV, pseudorapidity,  $|\eta| < 2.5$  and have to be isolated from energy depositions in the calorimeter and from reconstructed tracks. Jets are reconstructed with the anti- $k_t$  algorithm [20] with radius parameter  $R = 0.4$ , and are required to have  $p_T > 25$  GeV (30 GeV at 8 TeV). Central jets reach a pseudorapidity  $|\eta| < 2.5$  and forward jets, used in the  $t$ -channel analyses, reach  $|\eta| < 4.5$ . Information about jets containing  $b$  quarks is also used ( $b$ -tagging). A neural network combines lifetime-related information reconstructed from the tracks associated with each jet. The analyses use working points with 50 – 60% efficiency with a misidentification probability of 1/500. The missing transverse energy,  $E_T^{\text{miss}}$ , is reconstructed from the negative vector sum of the  $p_T$  of the physics objects and the transverse energy of unassociated calorimeter cells.

In CMS analyses, events are selected using single lepton triggers with isolation requirements at the trigger level, but also combined triggers, such as electron+ $b$ -jet trigger or dilepton triggers, are used. The physics objects are reconstructed from particle flow (PF) objects, that identify if tracks and energy depositions belong to electrons, muons, photons, charged or neutral hadrons and applies different calibrations accordingly. Leptons are required to be central ( $|\eta| < 2.5$ ) and to have  $p_T > 20 - 30$  GeV and isolation from other PF objects is also required. For the veto on additional leptons the  $p_T$ -requirement is usually lower than the  $p_T$  of the selected leptons. Jets are also built from PF objects with the anti- $k_t$  algorithm with radius parameter  $R = 0.5$ , and they must have  $p_T > 30$  GeV and can reach  $|\eta| < 4.5$ . The identification of jets from  $b$  quarks is using a threshold on a discriminator that is based on the secondary vertex reconstruction. The working point of the discriminator has  $\sim 60\%$  efficiency and a misidentification probability of 1/1000. The  $E_T^{\text{miss}}$  is reconstructed from the vector sum of the PF objects.

A commonly used variable is the transverse mass of the lepton- $E_T^{\text{miss}}$  system,  $m_T = \sqrt{2p_T E_T^{\text{miss}} [1 - \cos(\Delta\phi(\vec{l}, \vec{E}_T^{\text{miss}}))]}$ , with the  $p_T$  of the lepton, and the azimuthal angle  $\Delta\phi$

between the  $E_T^{\text{miss}}$  vector and the lepton vector,  $\vec{l}$ .

Top quarks decay virtually 100% to  $b$  quarks and a  $W$  boson. From the decay mode of the  $W$  boson (in case of a dilepton analysis, there are two  $W$  bosons) the events are classified into hadronic or leptonic modes. Most single-top analyses use the single-lepton mode using the lepton to trigger the event, while in the  $Wt$ -channel analysis the dilepton mode is preferred due to the lower background fraction.

### 3. Background estimations

The major background process for single top-quark analyses is top-pair ( $t\bar{t}$ ) production due to its large cross section and similarity of the decay chain. This background's shape is obtained from Monte-Carlo (MC) simulations while its normalisation is obtained from  $t\bar{t}$  dominated regions and varied within the theoretical cross-section uncertainty.

The next important background is  $W$ -boson production in association with additional jets ( $W$ +jets, light flavour and heavy flavour jets). The ATLAS analyses described here either simultaneously fit the normalisation of this background with the signal in the  $E_T^{\text{miss}}$  distribution or estimate it with the tag-counting method. In this method the overall normalisation is taken from  $W$ +jets dominated data samples and the fraction of  $W$ +jets events that contain jets from heavy-flavour decays are then estimated by comparing data events with and without the  $b$ -tag requirement.

CMS analyses described here use the shape and the normalisation of data events from a sideband of the analysis (see Section 4) that is dominated by  $W$ +jets events. After the subtraction of non- $W$ +jets events using MC samples, these events are used to model the  $W$ +jets background in the signal region.

$Z$ -boson production with associated jets is an important background for analyses in the dilepton final state. ATLAS analyses scale the MC events by comparing data to MC yields in sidebands of a 2D distribution in  $E_T^{\text{miss}}$  and the dilepton invariant mass (see Section 5). Some corrections are applied to account for non- $Z$ -boson background contributions. The CMS analyses correct the  $E_T^{\text{miss}}$  distribution, so that it agrees with data in the peak region.

The multijet background, in which a jet is misidentified as a lepton, is modelled in the ATLAS single-top analysis with two methods. The jet-electron model obtains shape templates for both the electron and the muon channel from events in which jets with electron-like energy depositions in the calorimeter are treated as electrons. The normalisation is taken from a fit to the  $E_T^{\text{miss}}$  data distribution after the preselection. The second method, the matrix method, uses equations that connect the number of selected data events to their sources of events with real and misidentified leptons for two definitions of the leptons. The efficiencies for real and misidentified leptons to pass the looser or both lepton definitions criteria that enter the method were determined in separate control regions dominated by the respective lepton types.

In the CMS analyses, the multijet background is modelled with template distributions from events using a looser lepton definition and that are dominated by multijet events. The normalisation is then determined from a fit to either the  $E_T^{\text{miss}}$  distribution (electron channel) or the  $m_T$  distribution (muon channel) before the cut on the respective variable in the analysis.

### 4. $t$ -channel cross-section measurement and single $t$ - and $\bar{t}$ -quark production cross-section ratio

The cross section of the single-top  $t$ -channel has been measured at both centre-of-mass energies, 7 TeV and 8 TeV. Since  $t$ -channel events contain typically forwards jets from the scattered initial parton, jets with  $|\eta| < 4.5$  are used.

The ATLAS analysis at  $\sqrt{s} = 7$  TeV uses  $1.04 \text{ fb}^{-1}$  of data [12]. It employs a multivariate analysis (MVA) that uses a neural network (NN) to separate the signal from background events in events with 2 and 3 jets. The multijet background is obtained from the jet-electron model,

while the  $W$ -boson and  $t\bar{t}$  processes are normalized during the signal extraction. To suppress the multijet background, events are required to have  $m_T + E_T^{\text{miss}} > 60$  GeV. The NN has been trained on the 12 (18) highest ranked variables in events with 2 (3) jets and exactly one  $b$ -tagged jet. The NN output distribution can be seen in Fig. 2(a). Among the highest ranked variables is the invariant mass of the lepton- $b$ -jet-neutrino system as depicted in Fig. 2(b). The cross section is determined from a maximum likelihood fit on the full output of the NN. The result is summarised in Table 2. This analysis has been cross checked with a cut-and-count analysis and also with another multivariate analysis using a boosted decision tree (BDT). The largest systematic uncertainties for this analysis are due to the modelling of the initial- and final-state radiation (ISR/FSR) and of the  $b$ -tagging.

With the full 7 TeV dataset of  $4.7 \text{ fb}^{-1}$  integrated luminosity and a similar analysis strategy, the ratio of single  $t$ - and  $\bar{t}$ -quark cross sections has been measured [14]. NNs have been trained separately for events with a positive or negative charged lepton. The total cross section is compatible with the previous result and the ratio of the cross section is  $R = 1.81 \pm 0.10$  (stat.)  $\pm 0.20$  (syst.). This result is shown in Fig. 2(c) alongside predictions using different PDF sets. The largest systematic uncertainties come from the background normalisation, ISR/FSR, multijet-background modelling and the jet energy scale.

For the analysis at  $\sqrt{s} = 8$  TeV with  $5.8 \text{ fb}^{-1}$  of data a similar strategy has been used [13]. Due to the more challenging pile-up conditions present in this dataset, tighter requirements on the jets and event variables are imposed. Jets are only selected if they have  $p_T > 30$  GeV and events need to satisfy  $E_T^{\text{miss}} > 30$  GeV and  $m_T > 50$  GeV. The background is modelled with the same methods as in the previous analysis. NNs were trained with 11 variables on events with 2 and 3 jets, separately. The largest systematic uncertainties for this analysis remain the modelling of the ISR/FSR radiation and of the  $b$ -tagging. The result is summarised in Table 2.

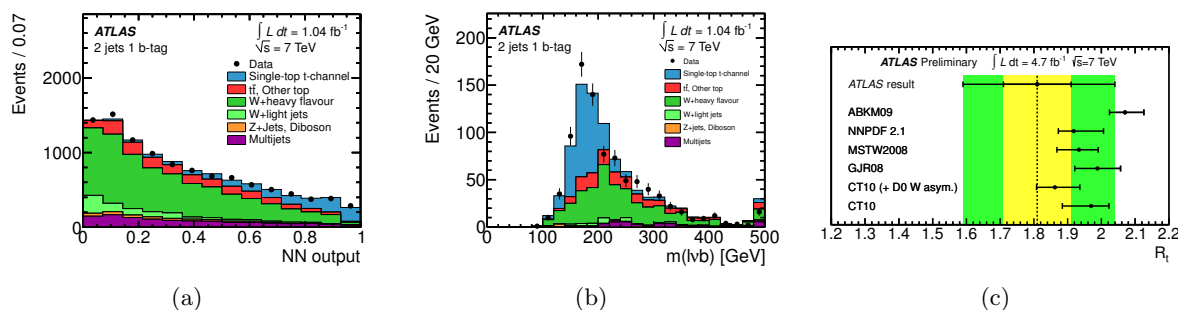


**Figure 2.** Selected ATLAS 7 TeV  $t$ -channel cross-section measurement figures showing (a) the NN output for events with 2 jets [12], (b) one of the most sensitive variables for the neural network, the invariant mass of the lepton- $b$ -jet-neutrino system for events with 2 jets [12] and (c) the measured ratio of single  $t$ - and  $\bar{t}$ -quark cross-section in comparison with predictions using different PDF sets [14].

The  $t$ -channel cross-section measurement performed by CMS at  $\sqrt{s} = 7$  TeV uses  $1.17 \text{ fb}^{-1}$  (muon channel) and  $1.56 \text{ fb}^{-1}$  (electron channel) data [17]. Events are required to have  $E_T^{\text{miss}} > 35$  GeV (electron channel) or  $m_T > 40$  GeV (muon channel) and to have exactly one  $b$ -tagged jet. The measurement combines the result from three analyses with the BLUE method [21]. Selected output distributions can be found in Fig. 3. Common to all analyses is the multijet-background estimation using a template from a multijet enriched region. The first analysis performs a maximum likelihood fit on the full range of the  $|\eta_{j'}|$  distribution where  $j'$  is the highest  $p_T$  non-tagged jet. A signal region with the requirement  $130 \text{ GeV} < m_{l\nu\nu} < 220 \text{ GeV}$  is defined to further enhance the signal.  $W$ +jets events are modelled from the sidebands. In the

likelihood fit, the  $W$ +jets,  $Z$ +jets and diboson samples are combined into a single background template. The other templates are from the signal,  $t\bar{t}$  events and from the multijet template. The NN analysis uses 6 events regions that have 2, 3 and 4 jets with 1 or 2  $b$ -tagged jets, respectively. For the electron (muon) channel 38 (37) variables are used. A BDT analysis uses the same event regions, but it is only trained on events with 2 and 3 jets and 1  $b$ -tagged jet with 11 observables. Both MVAs determine the cross section with a Bayesian method that uses a flat prior for the signal strength and Gaussian priors to include the systematic uncertainties as nuisance parameters. The theoretical uncertainties are not included as nuisance parameters and treated separately. The largest uncertainties after the combination are the statistical uncertainties, followed by the uncertainty on the  $W$ +jets normalisation and the generator uncertainties.

For the analysis at  $\sqrt{s} = 8$  TeV using  $5.0 \text{ fb}^{-1}$  only the single muon topology and the fit on the  $|\eta_{j'}$  distribution is used [18]. Similarly to the ATLAS analysis, the harsher pile-up conditions required adjustments to the object selection: for example the trigger threshold has been raised, the lepton is required to have  $p_T > 26$  GeV and  $|\eta| < 2.1$  and tighter isolation requirements. Jets in the event are required to have  $p_T$  larger than 40 GeV and events must have  $m_T > 50$  GeV. The background determination strategy is more elaborate and it fits the multijet template separately in the signal and sideband region. The  $t\bar{t}$  shape is taken from events with 3 jets of which 2 jets have to be  $b$ -tagged. The largest uncertainty arise from statistical limitations of the selected data sample, the jet energy scale and the uncertainty in the  $t$ -channel MC generator. All results are summarised in Table 2.

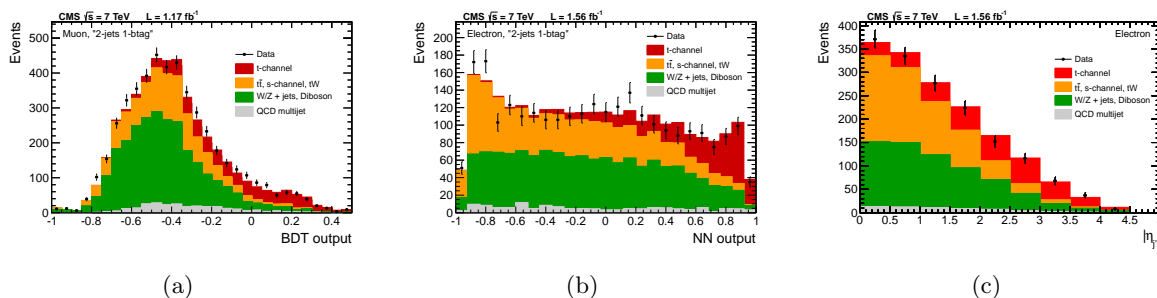


**Figure 3.** Selected output distributions of the analyses that were combined for the 7 TeV  $t$ -channel analysis with CMS [17], (a) the BDT output for events with 2 jets and a muon, (b) the NN output for electron events with 2 jets and (c) the  $|\eta_{j'}$  distribution of the hardest non-tagged jet.

**Table 2.** Summary of the single top-quark cross-section measurements and  $|V_{tb}|$  determinations for both experiments, ATLAS and CMS.

|                  | $t$ -channel [pb]  | $ V_{tb} ,  V_{tb}  @95\text{CL}$ for $ V_{tb} $ in $[0, 1]$ |
|------------------|--|--|
| ATLAS 7 TeV [12] | $83 \pm 4(\text{stat.}) \pm 20(\text{syst.})$  | $1.13 \pm 0.14, > 0.75$                                      |
| ATLAS 8 TeV [13] | $95 \pm 2(\text{stat.}) \pm 18(\text{syst.})$  | $1.04 \pm 0.11, > 0.80$                                      |
| CMS 7 TeV [17]   | $67 \pm 4(\text{stat.}) \pm 3(\text{syst.}) \pm 4(\text{theo.}) \pm 2(\text{lumi.})$ | $1.02 \pm 0.05 \pm 0.02(\text{theo.}), > 0.92$               |
| CMS 8 TeV [18]   | $80 \pm 6(\text{stat.}) \pm 11(\text{syst.}) \pm 4(\text{lumi.})$                    | $0.96 \pm 0.08 \pm 0.02(\text{theo.}), > 0.81$               |

### 5. $Wt$ -channel cross-section measurement

The ATLAS  $Wt$ -channel cross-section analysis uses  $2.05 \text{ fb}^{-1}$  of data at  $\sqrt{s} = 7$  TeV [15]. The events are selected to have at least one central jet and no  $b$ -tagging requirement is imposed on the

events. To reject background events,  $E_T^{\text{miss}} > 50$  GeV and a cut on the angle between the leptons and the  $E_T^{\text{miss}}$  vector is required. In addition for the  $ee$  and  $\mu\mu$  events, the invariant dilepton mass has to be outside of the  $Z$ -boson mass window. The  $Z$ -boson background normalisation in the signal region is determined as described in Section 3. The cross section is obtained from a profile likelihood method on the output of a BDT that can be seen in Fig. 4. The most sensitive variable here is the  $p_T$  of the system, which is the scalar sum of the  $p_T$  of all physics objects and  $E_T^{\text{miss}}$ . The BDTs are trained separately for events with 1, 2 and  $\geq 3$  jets using 22 observables. The largest systematic uncertainties are from the jet energy scale uncertainty, the parton shower modelling and the MC generator modelling. The result of  $17 \pm 6$  pb presents an evidence of the single-top  $Wt$ -channel production at a level of  $3.3\sigma$  significance ( $3.4\sigma$  expected significance).

The CMS analysis uses  $2.04 \text{ fb}^{-1}$  of data at  $\sqrt{s} = 7$  TeV and requires in the selection at least one  $b$ -tagged jet [19]. The  $E_T^{\text{miss}}$  requirements are  $E_T^{\text{miss}} > 30$  GeV and  $E_{T, \text{tracker}}^{\text{miss}} > 30$  GeV, which is the  $E_T^{\text{miss}}$  using tracks only. Again, for the  $ee$  and  $\mu\mu$  events the invariant dilepton mass has to be outside of the  $Z$ -boson mass window. The  $t\bar{t}$  background is constrained in enriched sample regions with 2 jets and 1 and 2  $b$ -tagged jets, respectively. The  $E_T^{\text{miss}}$  in the  $Z$  boson MC sample is corrected as described in Section 3. A binned likelihood fit to a BDT output, which is shown in Fig. 4, is performed in all signal and control regions to extract the cross section. The largest uncertainties on the signal modelling comes from statistical uncertainties, uncertainties on the jet energy scale and on the matrix-element/parton-shower matching threshold. The result of  $16 \pm 5$  pb corresponds to an evidence of the single-top  $Wt$ -channel production at CMS at a level of  $4.0\sigma$  significance ( $3.6\sigma$  expected significance). All results are summarised in Table 3.

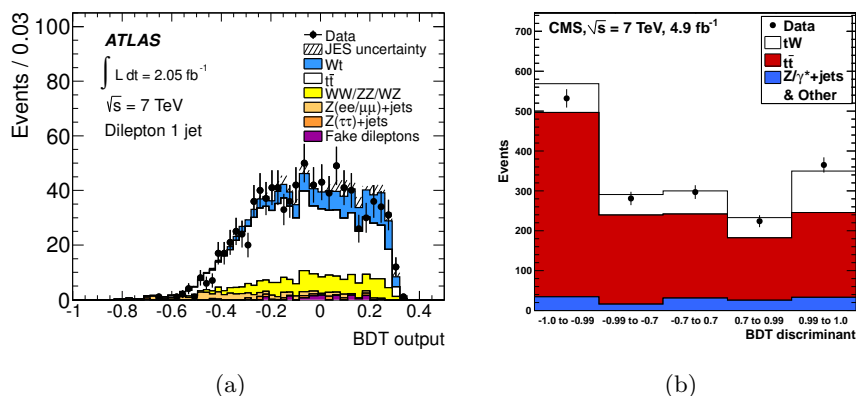


**Figure 4.** Selected BDT output distributions for the  $Wt$ -channel cross-section measurement, (a) the output for the ATLAS analysis for events with 1 jet [15] and (b) the output distribution for the CMS analysis [19].

## 6. $s$ -channel cross-section measurement

An attempt to measure the  $s$ -channel cross-section was only performed by ATLAS [16]. The analysis uses  $0.70 \text{ fb}^{-1}$  of data at  $\sqrt{s} = 7$  TeV, employing a cut-and-count method. Events are required to have exactly two central jets with exactly one  $b$ -tagged jets. These stringent jet requirements are necessary to suppress the largest background processes. To reduce the multijet background,  $E_T^{\text{miss}} > 25$  GeV and  $m_T + E_T^{\text{miss}} > 60$  GeV are also required. The  $W$ +jets background is estimated with the tag-counting method and the multijet background is estimated with the jet-electron model. The cut-based analysis uses a sequence of cuts optimized for best statistical significance. The cuts include several mass constraints on the mass of the reconstructed top and jets, the  $p_T$  of the jets and angular distances between the  $b$ -jet/jet-system

and the lepton. A likelihood ratio method on the number of expected events is used to extract a cross-section limit. So far no evidence of single-top  $s$ -channel production have been found at ATLAS. The major uncertainties are from the limited data and MC statistics and the MC generator uncertainties.

**Table 3.** Summary of the single top-quark cross-section measurements for the  $Wt$ - and  $s$ -channel and  $|V_{tb}|$  determinations for both experiments, ATLAS and CMS.

|   | $Wt$ -channel  | $s$ -channel                               |
|---|--|--|
| ATLAS 7 TeV [15, 16]  | $17 \pm 3(\text{stat.}) \pm 5(\text{syst.}) \text{ pb @ } 3.3\sigma$ | $< 26.5(\text{expected } 20.5) \text{ pb}$ |
| $ V_{tb} $  | $1.03^{+0.16}_{-0.19}$   |  |
| CMS 7 TeV [19]  | $16^{+5}_{-4} \text{ pb @ } 4.0\sigma$                               |  |
| $ V_{tb} ,  V_{tb}  \text{ @95CL for }  V_{tb}  \text{ in } [0, 1]$ | $1.01^{+0.16}_{-0.13} \pm 0.04(\text{theo.}), > 0.79$                |  |

## 7. Summary

The status of measurements of single top-quark production at the LHC has been presented here. The analyses at  $\sqrt{s} = 7$  TeV use up to the full 2011 data set and the analysis at  $\sqrt{s} = 8$  TeV use approximately a quarter of the available data in 2012. The  $t$ -channel cross-section has been measured at ATLAS and CMS for both centre-of-mass energies of 7 TeV and 8 TeV. These measurements are already limited by systematic uncertainties and precision measurements of the cross section will need to constrain the systematic uncertainties even more. With this clean selection of  $t$ -channel single-top events the measurements of the properties of single top-quark production can begin. Both experiments have found first evidence for  $Wt$ -channel production, which had not been observed before, at  $\sqrt{s} = 7$  TeV at  $3.3\sigma$  and  $4.0\sigma$  level of significance for ATLAS and CMS, respectively. For this channel, characterised by an almost irreducible  $t\bar{t}$  background, the statistical and systematical uncertainties are at the same level. With more data becoming available at  $\sqrt{s} = 8$  TeV a discovery seems to be possible in the near future. All measurements also determine the CKM-matrix element  $|V_{tb}|$  and it seems to be compatible with the expectation from the SM. For the subleading process, the  $s$ -channel, a cross-section limit has been set by ATLAS and this analysis is clearly dominated by statistical uncertainties. So far, the measured cross sections show good agreement with the predictions by the SM.

## References

- [1] Kidonakis N 2011 *Phys. Rev. D* **83** 091503 (Preprint arXiv:1103.2792[hep-ph])
- [2] Kidonakis N 2010 *Phys. Rev. D* **82** 054018 (Preprint arXiv:1005.4451[hep-ph])
- [3] Kidonakis N 2010 *Phys. Rev. D* **81** 054028 (Preprint arXiv:1001.5034[hep-ph])
- [4] Aliev M, Lacker H, Langefeld U, Moch S, Uwer P *et al.* 2011 *Comput. Phys. Commun.* **182** 1034–1046 hATHOR version 1.2 is used. (Preprint 1007.1327)
- [5] Tait T M and Yuan C P 2000 *Phys. Rev. D* **63** 014018 (Preprint hep-ph/0007298)
- [6] ATLAS Collaboration 2012 *Phys. Rev. Lett.* **109** 081801 (Preprint 1205.1016)
- [7] CMS Collaboration 2012 (Preprint 1208.0956)
- [8] ATLAS Collaboration 2013 (Preprint 1301.1583)
- [9] ATLAS Collaboration 2012 *Phys. Lett. B* **712** 351–369 (Preprint 1203.0529)
- [10] ATLAS Collaboration 2008 *J. Inst.* **3** S08003
- [11] CMS Collaboration 2008 *JINST* **3** S08004
- [12] ATLAS Collaboration 2012 *Physics Letters B* **717** 330–350 (Preprint 1205.3130)
- [13] ATLAS Collaboration ATLAS-CONF-2012-132 URL <https://cds.cern.ch/record/1478371>
- [14] ATLAS Collaboration ATLAS-CONF-2012-056 URL <http://cds.cern.ch/record/1453783>
- [15] ATLAS Collaboration 2012 *Phys. Lett. B* **716** 142 (Preprint 1205.5764)
- [16] ATLAS Collaboration ATLAS-CONF-2011-118 URL <http://cds.cern.ch/record/1376410>
- [17] CMS Collaboration 2012 Submitted to JHEP (Preprint 1209.4533)
- [18] CMS Collaboration CMS-PAS-TOP-12-011 URL <http://cds.cern.ch/record/1478935>

- [19] CMS Collaboration 2012 *Phys. Rev. Lett.* (*Preprint* 1209.3489)
- [20] M Cacciari, G P Salam and G Soyez 2008 *JHEP* **0804** 063 (*Preprint* 0802.1189)
- [21] Lyons L, Gibaut D and Clifford P 1988 *Nucl.Instrum.Meth.* **A270** 110